Greenhouse Warming Potentials from the Infrared Spectroscopy of Atmospheric Gases

Matthew J. Elrod
Department of Chemistry, Hope College, Holland, MI 49423; *elrod@hope.edu*

Background

The recent climate conference in Kyoto, Japan, resulted in an agreement by industrialized nations to reduce emissions of six key greenhouse gases (GHGs) to about 5% below 1990 emissions levels by the year 2012 (*1*). In order to evaluate the potential contribution of each individual GHG to global warming, the greenhouse warming potential (GWP) was devised to aid in the identification of particularly effective GHGs. This scale is regularly used by policy makers to guide decisions concerning the control of emissions of these substances. The six substances included in the Kyoto agreement are species whose atmospheric concentrations are rapidly increasing, that possess extremely large GWPs, or both. The GWP depends on the strength with which a given species absorbs infrared radiation, the spectral location of its absorbing wavelengths, and the atmospheric lifetime of the species. Because the GWP of a GHG depends directly on the infrared spectrum of that species, the use of infrared spectroscopy to identify GHGs is centrally important in the effort to understand the impact of human activities on global climate change.

Because of student interest in the global warming issue and the wide availability and use of Fourier transform infrared (FTIR) spectroscopy in the undergraduate curriculum, many physical chemistry (and some general chemistry) courses now include laboratory exercises concerning the identification of GHGs. However, most such laboratory courses simply involve the measurement of the infrared spectrum of several different atmospheric gases, and GHGs are *qualitatively* identified according to whether they absorb radiation in the infrared region. In other words, a greenhouse gas is identified if it absorbs somewhere in the 400–4000 cm^{-1} region. This sort of analysis is misleading, since the position and strength of the absorptions and the atmospheric lifetime of the species can profoundly affect its actual GWP. Because this qualitative analysis does not reveal which specific properties of GHGs are most important, the student is not able to see the direct connection between the infrared spectrum that is obtained and how such data are ultimately used to influence public policy decision-making.

To illustrate the major influence that specific molecular properties can have on the calculated GWP, it is particularly useful to consider the GWPs of molecules containing C–F bonds. It is well known that C–F vibrational transitions possess extremely large infrared absorption cross sections, which have a relatively obvious effect on the GHG potential of those species. However, there are two other, more subtle, properties of the C–F bond that can greatly add to the molecule's ability to act as a greenhouse gas: (i) the C–F bond is relatively unreactive in the oxidizing environment of the atmosphere, allowing these species to have very long residence lifetimes in the atmosphere, and (ii) several of the fundamental vibrational frequencies of molecules containing C–F bonds occur in intense regions of the earth's blackbody spectrum that are not already absorbed by naturally occurring gases such as CO_2, H_2O, and O_3 (the "window" region of 800–1200 cm^{-1}) (*2*). Due to these three particular characteristics of C–F bond-containing species, it is not unexpected that two of the six classes of GHGs included in the Kyoto agreement contain C–F bonds. A *numerical* measure, such as the GWP, distinguishes the more effective GHGs from the less effective GHGs, and makes the connection between the infrared spectroscopy of GHGs and the use of such data in the development of public policy decisions such as those made at the Kyoto conference.

Overview of the Exercise

It is the purpose of this work to demonstrate how an easily obtained infrared spectrum and a simple spreadsheet analysis can be used to determine relatively accurate GWPs for many of the GHGs included in the Kyoto agreement. Through this exercise, students learn an additional level of sophistication in the interpretation of infrared spectra (i.e., the determination of absolute absorption cross sections) and apply these data to a simple model, which can be used to generate GWPs. From the calculated GWPs, students gain a better understanding of the spectral characteristics of particularly effective GHGs and can rationalize the choice of the six GHGs targeted for emission reduction at the Kyoto conference.

For this experiment, N_2O (emitted by agricultural processes), CH_4 (emitted by agricultural and fossil fuel production processes), SF_6 (emitted by various manufacturing processes), CF_3CH_2F (the current coolant in automobile air conditioning systems) and CH_2Cl_2 (a common organic solvent) were chosen for study for practical (cheap, easy and safe to handle) and for illustrative (widely varying GWPs) reasons.

Infrared Spectra

An infrared gas cell (10-cm path length) equipped with KBr windows was filled with the gas sample. The pressure of the sample was chosen so that the maximum absorption in the 500–1500 cm^{-1} region was about 1.0, to ensure good Beer's law behavior. The gases N_2O, CH_4, SF_6, CF_3CH_2F, and CH_2Cl_2 were analyzed at pressures of 60, 60, 4, 6, and 8 torr, respectively. Absorption spectra were obtained on a Midac FTIR spectrometer with the resolution set to 2 cm^{-1}. Using the FTIR software, all of the absorption features in the range from 500 to 1500 cm^{-1} were integrated in 10-cm^{-1} intervals and recorded (although more approximate integration methods would suffice). The spectrum of CF_3CH_2F is shown in Figure 1 and is the object of the following analysis.

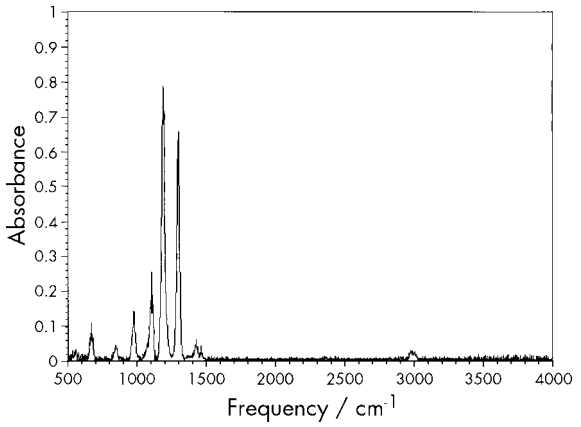

Figure 1. Infrared spectrum of CF_3CH_2F (6 torr).

Narrow-Band Radiative Forcing Model and Greenhouse Warming Potentials

The surface temperature of Earth is higher than can be predicted simply from the flux of visible light incident on the earth's surface. The earth also acts as a blackbody radiator, but because it possesses a much lower surface temperature than the sun, it primarily emits infrared light.

Greenhouse warming arises when the atmosphere traps infrared radiation that would otherwise be emitted into space. As mentioned above, the GWP depends on the number, strength, and position of a GHG's absorption bands and on its atmospheric lifetime. The overlap of the infrared spectrum of the GHG and the blackbody infrared radiation emitted by the earth's surface (more accurately, the portion of the blackbody spectrum that is not absorbed by naturally occurring atmospheric gases) is referred to as the radiative forcing capacity of the GHG. Simply put, the radiative forcing capacity is the amount of energy per unit area per unit time that the GHG absorbs that would otherwise be lost to space. The GWP is the radiative forcing capacity of the GHG weighted by the residence time of the species in the atmosphere.

Pinnock et al. have proposed a narrow-band radiative forcing model that requires only simple spreadsheet calculations to estimate the radiative forcing of a GHG from the integrated absorption cross sections obtained from the infrared spectrum of the GHG (*3*). In this narrow-band model, the radiative forcing per unit cross section for the average Earth sky (i.e., including clouds) is parameterized in 10-cm^{-1} intervals for a 1-part-per-billion by volume (ppbv) increase in the GHG. The radiative forcing is peaked around 900 cm^{-1} (as predicted by the blackbody temperature of the earth) with several "holes" in the spectrum caused by absorptions of CO_2, H_2O, and O_3 and is shown in Figure 2. The radiative forcing for the GHG in watts per square meter for a 1-ppbv increase is given by

$$RF = \sum_{i=1}^{100} \sigma_i F_i^{\sigma} \qquad (1)$$

where F_i^{σ}, in units of W m^{-2} $(cm^{-1})^{-1}$ $(cm^2$ $molecule^{-1})^{-1}$, is the radiative forcing per unit cross section per inverse centimeter for the spectral interval i for the average Earth sky and σ (cm^2 $molecule^{-1}$ cm^{-1}) is the integrated cross section over each 10-cm^{-1} spectral interval from the infrared spectrum of the GHG. The F_i^{σ} values are tabulated in Pinnock et al. (*3*). For this implementation, the region from 500 to 1500 cm^{-1} was used, resulting in 100 10-cm^{-1} bands. Although most of the earth's blackbody spectrum falls in this region, the lower limit of 500 cm^{-1} is actually dictated by the transmission limit of the KBr windows used in the infrared cell. Pinnock et al. list F_i^{σ} values for the more inclusive range 0–2500 cm^{-1}. The average cross section is obtained from the integrated absorption data via Beer's law

$$\sigma = \frac{A^{\text{int}}}{l\,n} \qquad (2)$$

where A^{int} is the integrated absorption data for the 10-cm^{-1} interval in cm^{-1}, l is the path length of the IR cell in cm, and n is the number density of the GHG in molecules cm^{-3}.

The potential of 1 kg of a compound A to contribute to radiative forcing relative to that of 1 kg of a reference compound R is referred to as the greenhouse warming potential (*4*)

$$\text{GWP} = \frac{RF^{\text{A}} \times \int_0^{\text{TH}} \text{A}(t)\,dt}{RF^{\text{R}} \times \int_0^{\text{TH}} \text{R}(t)\,dt} \qquad (3)$$

where TH is the time horizon, RF^{A} is the radiative forcing resulting from a 1-kg increase of compound A, A(t) is the time decay of a pulse of compound A, and RF^{R} and R(t) are the comparable quantities for the reference. The most common reference compound is CO_2 and it will serve as the reference compound in the analysis described here. The time horizon is the amount of time to be considered in comparing the greenhouse potential of the GHG to that of the reference compound. For example, if a GHG has an atmospheric lifetime longer than CO_2, it will have a larger GWP at longer time horizons than short ones, since CO_2 will be removed from the atmosphere at a faster rate. Although the actual form of the time decays for the relevant chemical species can be complicated (particularly for CO_2), a simple exponential decay function will be used in the following analysis to allow for an easily integrable form of eq 3. Because the radiative forcing function above is derived on a per-molecule basis, eq 3 must be modified to place the radiative forcing on a per-mass basis. Therefore, the form of the GWP to be used in this analysis is

$$\text{GWP} = \frac{RF^{\text{GHG}} \times \left(\frac{1000}{\text{MW}^{\text{GHG}}}\right) \times \int_0^{\text{TH}} e^{-t/\tau^{\text{GHG}}}\,dt}{RF^{\text{CO}_2} \times \left(\frac{1000}{\text{MW}^{\text{CO}_2}}\right) \times \int_0^{\text{TH}} e^{-t/\tau^{\text{CO}_2}}\,dt} \qquad (4)$$

where MW is the molecular mass in g mol^{-1} and τ is the atmospheric lifetime in years for the GHG and CO_2, respectively. To summarize, the required information needed to calculate the GWP includes the path length of the IR cell, the partial pressure of the GHG in the cell, the atmospheric lifetime of the GHG, the molecular weight of the GHG, and the integrated absorption data in 10-cm^{-1} intervals.

Approximate Nature of the Narrow-Band-GWP Model

The narrow-band-GWP model described above relies on a number of approximations that limit the quantitative accuracy of the method. Although a consideration of these approximations is not necessary to obtain meaningful results from the model, it is instructive to explore these details because they reveal the inherently complex process that is involved in the modeling of global climate change. The GWP relation defined here (eq 4) uses an exponential decay approximation for the time pulse of GHGs. This approximation is poor for CO_2 (whose time pulse is characterized by three quite different rates of decay [*4*]) and may be inappropriate for other gases, as well. In fact, the difficulty in determining the lifetime of a GHG is often the major source of uncertainty in the calculation of the GWP. The defined lifetime is also predicated on the approximation that the GHG is "well mixed" globally (latitude, longitude, and altitude), so that GHGs with longer lifetimes are more adequately modeled. The determination of the radiative forcing function is approximate in that it assumes the condition of optical thinness (i.e., Beer's law applies: absorption is linearly proportional to the concentration of a GHG). For example, in the regions of the blackbody spectrum where GHG absorption is already significant, saturation effects lead to a situation where absorption is more nearly proportional to the logarithm of the concentration (*3*). This is the explanation for the modeling result that a doubling in CO_2 concentration leads to much less than a doubling in the radiative forcing from CO_2 (and thus, approximately, less severe global temperature increases due to rising CO_2 levels) (*4*). The absolute integrated absorption cross sections determined in this analysis may also lead to uncertainty in the GWP results because they were obtained from spectra measured at 2-cm^{-1} resolution. For molecules with large rotational constants (such as CH_4), there can be significant error in the determination of the integrated cross sections from absorbance measurements, although, in principle, these errors can be reduced by the use of pressure-broadening gases (*5*).

Spreadsheet Calculations and Results

The GWP is easily calculated using any spreadsheet program. The spreadsheet method results in the generation of five columns and 100 rows of data for a GWP calculation over the range 500–1500 cm^{-1}. The first column of data is the center frequency ν_c of each 10-cm^{-1} absorption band and the second column contains the F_i^{σ} values from Pinnock et al. (*3*). These columns of data are the same for the analysis of all GHGs. The third column of data contains the integrated absorption areas obtained from the infrared spectrum of the GHG.

It is instructive to plot the F_i^{σ} and σ vs ν_c to visually study the overlap of the absorption bands and the relevant portions of Earth's blackbody spectrum (see Fig. 2 for results obtained for CF_3CH_2F). It is clear from this figure that CF_3CH_2F is a very effective GHG, as it possesses seven strong vibrational bands in the 500–1500 cm^{-1} region. In particular, the strength of these bands is best appreciated by comparing them to the relatively weak C–H stretching bands located near 3000 cm^{-1}, as shown in Figure 1. Note that the 666-cm^{-1} band does not significantly contribute to greenhouse warming because most of the infrared radiation in that region is already absorbed by the 667-cm^{-1} bending vibration of CO_2.

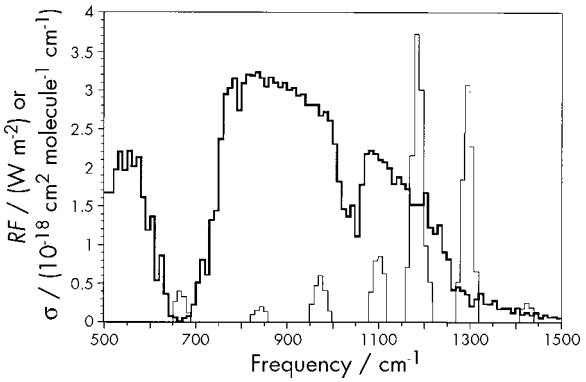

Figure 2. Narrow-band radiative forcing (RF) for average Earth sky (bold line) and integrated absolute absorption cross section (σ) for CF_3CH_2F (thin line).

Table 1. Greenhouse Warming Potentials Determined by the Narrowband Radiative Forcing Model

GHG	Lifetime/years	Time Horizon/years		
		20	100	500
		GWP		
CO_2[a,b]	150	1	1	1
CH_4[a]	15	37	13	6
N_2O[a]	120	93	88	77
CF_3CH_2F[a]	14	729	246	124
SF_6[a]	3200	1737	2200	5220
CH_2Cl_2	0.41	11	2.9	1.5

[a]Emissions regulated by Kyoto agreement.
[b]By definition, the GWP is 1 for CO_2 for all time horizons.

The fourth and fifth columns contain the σ (calculated from eq 2) and the individual components of the *RF* (calculated from eq 1), respectively. The *RF* is then calculated by summing the fifth column and the GWP is calculated from the analytical form of eq 4, the radiative forcing and atmospheric lifetime for CO_2 (1.1×10^{-5} W m^{-2} and 150 years, respectively) and the atmospheric lifetime for the GHG (see Table 1 for the atmospheric lifetimes of several GHGs or see Seinfeld et al. [*4*] for a larger list). Both Excel and Mathcad software have been used to carry out the GWP calculations. The design of the Excel spreadsheet explicitly follows the discussion given above. Sample documents in both formats are available for CF_3CH_2F at *http://www.chem.hope.edu/~elrod/mathcad/gwp.mcd* (Mathcad, Version 6.0+) and *http://www.chem.hope.edu/~elrod/mathcad/gwp.xls* (Excel, Version 7.0).

Table 1 contains the lifetimes for the GHGs studied here and the GWP results obtained for 20-, 100-, and 500-year time horizons. These results are in reasonable agreement (within a factor of 2–3) with the results obtained by more rigorous treatments of the radiative forcing and atmospheric lifetimes, as discussed above. On the basis of these results, students are able to *numerically* distinguish the more effective

Table 2. Atmospheric Abundances, Growth Rates, and Approximate Absolute Greenhouse Warming Effects

GHG	Atmospheric Abundance / ppbv	Growth Rate / (ppbv / year)	Growth Rate × GWP (20-year)	Ref
CO_2	356,000	1000	See text	*7*
CH_4	1,714	7	259	*7*
N_2O	310	0.7	65	*7*
CF_3CH_2F	1.48×10^{-3}	1.24×10^{-3}	0.90	*8*
SF_6	2×10^{-3}	1.5×10^{-4}	0.26	*9*

GHGs that are included in the Kyoto agreement (CH_4, N_2O, CF_3CH_2F, and SF_6) from the less effective GHG (CH_2Cl_2) that is not included in the Kyoto agreement. In addition, students are able to determine the *specific* features (strength, location, or numbers of IR absorption bands or atmospheric lifetime) of the GHG that lead to a particularly large or small GWP.

Discussion

It should be noted that ab initio methods have been used to estimate the absolute absorption cross sections needed for the narrow-band analysis described here (*6*). The use of such ab initio methods (in conjunction with visualization software) presents an additional learning opportunity in that it would allow students to investigate the specific modes that lead to enhanced greenhouse warming potentials, further demonstrating the specific molecular properties characteristic of GHGs.

It is important to recall that the GWP scale is a relative one, comparing the greenhouse warming potential of the GHG to that of carbon dioxide on a per mass basis. However, to evaluate the increasing contribution to greenhouse warming for each gas, the differing *absolute* growth rates of the greenhouse gases present in the atmosphere must be considered. For example, the preceding analysis shows that CO_2 is not a particularly effective GHG on a per mass basis, but it is well known that CO_2 is the most effective GHG on an absolute basis because of the extremely large growth rates of CO_2 in the atmosphere.

In Table 2, the atmospheric abundances, growth rates, and product of the GWP and the growth rate (an approximate measure of the increasing absolute greenhouse warming effect of each gas) of the actual GHGs used in this study are presented. This approximate measure of the yearly impact on greenhouse warming by increasing CO_2 is not appropriate because the condition of optical thinness clearly does not apply, and therefore this entry in the table is left empty. However, the table does make clear that gases with large GWPs and relatively small, but increasing, growth rates (such as SF_6 and CF_3CH_2F) can have a substantial impact on global warming even by comparison to gases with much larger growth rates (such as CO_2 and CH_4). Using the model presented here, students are easily able to *numerically* reproduce the scientific reasoning that supports the global effort to reduce greenhouse gas emissions.

Conclusions

To our knowledge, no other experiment in the chemical education literature incorporates calculations of greenhouse warming potential. The novel aspect of this approach is the use of infrared spectroscopic absorption information as applied to the topical problem of global climate change. Because the greenhouse warming potential is one of the greenhouse gas properties that are used in the public policy arena, students are motivated to understand the relationship between experimental data that are obtained and putting such data to use in policy making.

Acknowledgments

I acknowledge The Camille and Henry Dreyfus Foundation Faculty Start-up Grant Program for Undergraduate Institutions (SU-96-001) and the National Science Foundation CAREER Program (ATM-9874752) for support, and Will Polik for helpful suggestions.

Literature Cited

1. Hileman, B. *Chem. Eng. News* 1997, *75*(Dec 22) 20–22.
2. Shine, K. P. *J. Atmos. Sci.* 1991, *48*, 1513–1518.
3. Pinnock, S.; Hurley, M. D.; Shine, K. P.; Wallington, T. J.; Smyth, T. J. *J. Geophys. Res. Atmos.* 1995, *100*, 23227–23238.
4. Seinfeld, J. H.; Pandis, S. N. *Atmospheric Chemistry and Physics*; Wiley-Interscience: New York, 1998.
5. Freckleton, R. S.; Pinnock, S.; Shine, K. P. *J. Quant. Spectrosc. Radiat. Transfer* 1996, *55*, 763–769.
6. Papasavva, S.; Tai, S.; Illinger, K. H.; Kenny, J. E. *J. Geophys. Res.* 1997, *102*, 13643–13650.
7. *Scientific Assessment of Stratospheric Ozone: 1994*; WMO Global Ozone Research and Monitoring Project; World Meteorological Organization: Geneva, Switzerland, 1994.
8. Oram, D. E.; Reeves, C. E.; Sturges, W. T.; Penkett, S. A.; Fraser, P. J.; Langenfelds, R. L. *Geophys. Res. Lett.* 1996, *23*, 1949–1952.
9. Rinsland, C. P.; Mahieu, E.; Zander, R.; Gunson, M. R.; Salawitch, R. J.; Chang, A. Y.; Goldman, A.; Abrams, M. C.; Abbas, M. M.; Newchurch, M. J.; Irion, F. W. *Geophys. Res. Lett.* 1996, *23*, 2349–2352.